



## In Situ Kinetics Studies in All-Vanadium Redox Flow Batteries

Douglas Aaron,<sup>a</sup> Che-Nan Sun,<sup>b</sup> Michael Bright,<sup>a</sup> Alexander B. Papandrew,<sup>a</sup>  
Matthew M. Mench,<sup>c,d,\*</sup> and Thomas A. Zawodzinski<sup>a,b,\*\*,z</sup>

<sup>a</sup>Chemical and Biomolecular Engineering, University of Tennessee, Knoxville, Tennessee 37996, USA

<sup>b</sup>Physical Chemistry of Materials Group, Oak Ridge National Laboratory, Oak Ridge, Tennessee 37831, USA

<sup>c</sup>Department of Mechanical, Aerospace and Biomedical Engineering, University of Tennessee, Knoxville, Tennessee 37996, USA

<sup>d</sup>Emissions and Catalysis Research Group, Oak Ridge National Laboratory, Oak Ridge, Tennessee 37831, USA

We report results of polarization measurements resolved for the negative and positive electrodes of vanadium redox batteries (VRBs) using a dynamic hydrogen electrode in an operating battery cell. Electrochemical experiments with symmetric electrolyte feeds were also performed. Greater kinetic polarization is observed at the negative ( $V^{3/2+}$ ) electrode compared to the positive electrode ( $V^{5/4+}$ ), in contrast with previously reported ex situ measurements. For the positive electrode, the polarization in the low-current regime was modest and was not kinetically controlled. The relative rates of reaction are a surprise since it might be expected that the  $V^{3/2+}$  redox reaction is a simple outer-sphere electron transfer.

© 2013 The Electrochemical Society. [DOI: 10.1149/2.001303eel] All rights reserved.

Manuscript submitted September 12, 2012; revised manuscript received November 27, 2012. Published January 8, 2013.

Increasing demand for renewable energy, focused on intermittent sources such as wind and solar, has resulted in great interest in large-scale energy storage. Redox flow batteries (RFBs) are proposed to allow large-scale, low-cost electrical storage, enabling intermittent energy production technologies to take a greater share of the domestic energy portfolio.<sup>1</sup> To realize this goal, significant improvements are needed in RFB performance and cost.

A variety of processes can contribute to performance limitations in RFBs. At the cell level in the all-vanadium chemistry, reaction kinetics, ionic transport through electrodes and the separator, electronic contact resistance, and mass transport resistance into and out of the electrodes are all expected to reduce the power available from a RFB. Polarization curve analysis has been used in all-vanadium RFBs to aid in separating the above contributions to overpotential at varying operating currents.<sup>2</sup> It is quite important to assess the relative magnitude of these losses, particularly in the low current regime of high conversion efficiency. Generally, this region can be very strongly affected by kinetic limitations.

VRB reaction kinetics studies in the VRB cell itself are somewhat complicated by the need for a reference electrode. Thus, most investigations of kinetics to date were carried out using ex-situ methods, such as rotating disk electrode (RDE) voltammetry or stationary cyclic voltammetry (CV). Gattrell<sup>3</sup> observed Tafel slopes as high as 130–500 mV/decade and exchange currents ranging from  $\sim 0.2$  mA/cm<sup>2</sup> to  $\sim 7$  mA/cm<sup>2</sup> for the  $V^{5/4+}$  couple on a glassy carbon RDE. Suspicion of kinetic limitations has led some to treat the carbon electrodes to improve reaction rates, but with little appreciable improvement.<sup>4</sup> Recent work by Manahan<sup>5</sup> found that improved cell performance resulted from replacing the negative electrode carbon paper with higher surface area carbon paper; similar improvement was not realized when the positive electrode material was replaced. However, two-electrode in-situ tests suffer from the inability to definitively ascribe the observed losses or improvements to either the positive or negative electrode.

Inserting a reference electrode into the VRB single cell allows electrode kinetics measurements to be performed in-situ by separating individual electrode contributions to the observed loss after iR correction. Here we report our implementation of a dynamic hydrogen electrode as a reference electrode for a study focused on the low-current region of the polarization curve to probe the kinetics of the positive and negative sides of a VRB using carbon paper electrodes.

### Methods

**Cell construction.**— The RFB hardware used in this work was a modified direct methanol fuel cell with an active area of 5 cm<sup>2</sup> described in detail previously.<sup>6</sup> Single layers of untreated 10 AA carbon paper (SGL group) with a nominal thickness of 410  $\mu$ m and 328 cm<sup>2</sup> BET surface area<sup>7</sup> were used as electrodes on both sides of the cell. Temperature was maintained at 25°C via cartridge heaters on the cell. Two layers of Nafion 117 (Ion-Power) enabled the incorporation of a dynamic hydrogen electrode (DHE) into the cell,<sup>8</sup> as illustrated in Figure 1.

The electrolyte was 0.1 M vanadyl sulfate (Alfa Aesar) in 5.0 M sulfuric acid (Alfa Aesar). A state-of-charge (SoC) of 50% was used. Details of electrolyte preparation and charging are given in Aaron et al.<sup>6</sup> The 0.1 M vanadium concentration was lower than what is used in practical VFRBs but is a more thermally stable solution than obtained at higher concentration.<sup>9</sup> The electrolyte flow rate was 20 mL/min, corresponding to a maximum utilization of 7.5% at the highest measured current.

**Electrochemical measurements.**— Potentiostatic polarization curves were performed in the low current region – up to approximately 40 mA/cm<sup>2</sup> – to focus on kinetic control. All overpotentials were controlled with respect to the stable open circuit potential prior to the beginning of the experiment. To maintain a constant 50% SoC throughout a polarization measurement, 4 s steps of alternating polarity overpotential were applied. Figure 2 shows the applied potential at the  $V^{5/4+}$  electrode and the cell current vs. time, illustrating that a 4 s discharging step at, for example,  $-1$  mV overpotential was followed by a 4 s charging step at  $+1$  mV overpotential relative to the OCV. It is apparent that the ending OCV was the same as the starting OCV, indicating that the VRB SoC was unchanged throughout the course of the experiment. The current was sampled during the final 25% of each time step to exclude capacitive charging currents. The high frequency resistance (HFR) was measured using AC impedance at 10 mV r.m.s. amplitude at roughly 15 kHz. The areal specific resistance (ASR, or HFR\*area) on the positive side was 0.513  $\Omega$ -cm<sup>2</sup> and 0.519  $\Omega$ -cm<sup>2</sup> on the negative side. The whole cell ASR, measured from the positive to the negative electrode, was 1.07  $\Omega$ -cm<sup>2</sup>. These values were slightly larger for the symmetric cell experiments, described below.

A second set of experiments was performed to verify the polarization curve studies described above. In these, a symmetric cell was operated in which both sides of the battery were fed a 50% SoC  $V^{3/2+}$  or  $V^{5/4+}$  electrolyte. The electrolyte for both sides was contained in one external reservoir so that no SoC change could take place. Thus, for the  $V^{3/2+}$  symmetric cell,  $V^{2+}$  was oxidized to  $V^{3+}$  on one side

\*Electrochemical Society Active Member.

\*\*Electrochemical Society Fellow.

<sup>z</sup>E-mail: tzawodzi@utk.edu

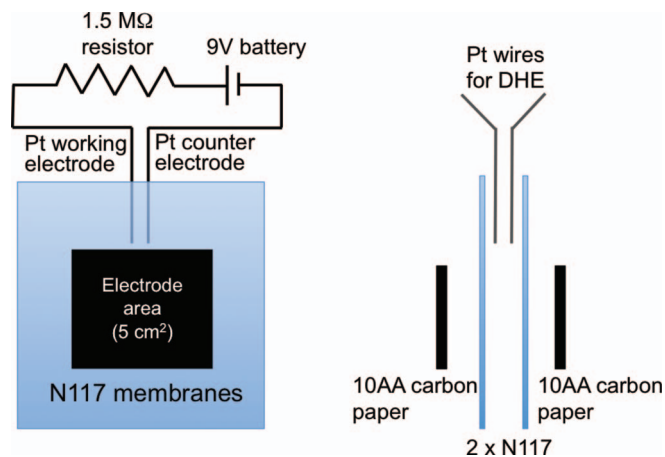


**Figure 1.** Placement of the DHE in the RFB (face view and side view on left and right, respectively). On the side view, the spacing between the tips of the Pt wires was  $\sim 1$  mm; the tips of the wires were  $\sim 1$  mm outside the active area of the electrodes.

while  $V^{3+}$  was reduced to  $V^{2+}$  on the other side (and similar for the  $V^{5/4+}$  symmetric cell).

The DHE was inserted between layers of Nafion 117. A steady current of  $6 \mu\text{A}$  flowed between the electrodes of the DHE. This provided a stable reference voltage over the course of several months of operation in the VRB. Within experimental error, identical HFR values were observed between the reference and each of the electrodes in the cell, indicating that the DHE provided a plausible reference when placed outside the electrode active area. The accuracy of the potential relative to reference electrode placement, the geometry of the system and the relative rates of reaction (secondary current distribution) were analyzed by He<sup>10</sup> and Liu.<sup>11</sup> To meet criteria suggested in these works, we placed the reference electrode far (relative to membrane thickness) outside the edge of either electrode. We also investigated the measured kinetics in both normal and symmetric cells, finding identical current-potential behavior.

## Results

Figure 3 shows charging and discharging polarization data for the positive and negative electrodes of the VRB. The negative electrode exhibited much greater overpotential at all cell current densities than the positive electrode. If the current response to overpotential is kinetically controlled, a plot of log current against overpotential should achieve a linear trend once the individual electrode reactions have been biased primarily in one direction (i.e. charging or discharging).

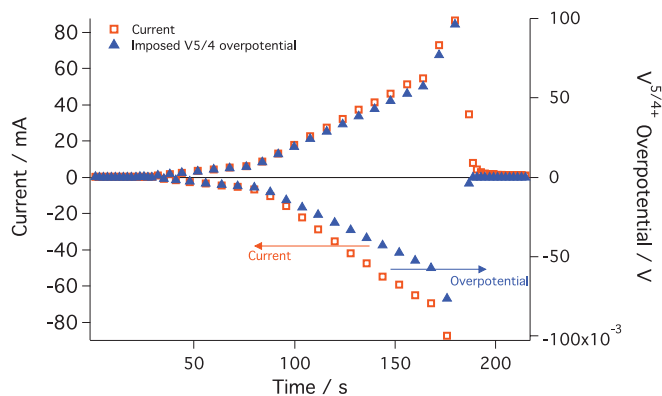


**Figure 2.** Current and potential profiles over time for the alternating charge-discharge polarization curves. Note that an ending overpotential of 0 V indicates that the VRB SoC was unchanged. The electrolyte was 0.1 M vanadium in 5.0 M  $\text{H}_2\text{SO}_4$ .

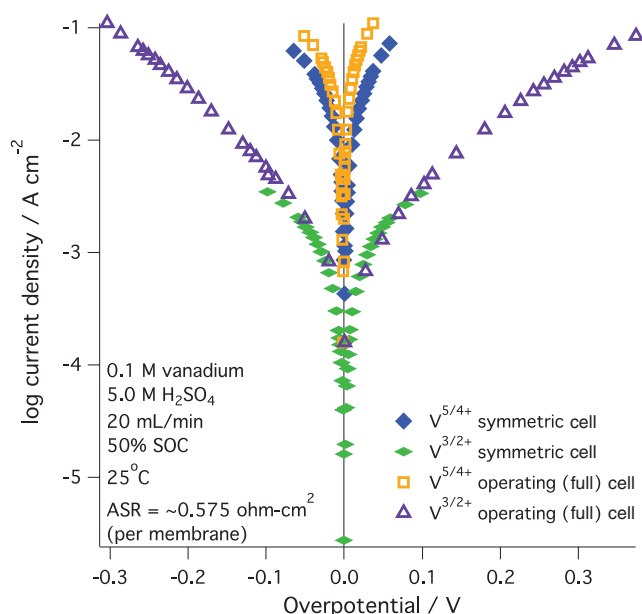


**Figure 3.** Kinetic region polarization data for VRB charging and discharging behavior. The electrolyte was 0.1 M vanadium in 5.0 M  $\text{H}_2\text{SO}_4$ .

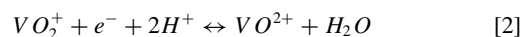
Construction of a Tafel plot in this manner allows kinetic parameters such as the Tafel slope and exchange current density to be obtained. The Tafel range spans approximately 1.2 decades of log current density for the full cell experiment. The exchange current density,  $j_0$ , is of particular interest since a higher  $j_0$  indicates faster kinetics.

The charging and discharging curves for the negative electrode yielded Tafel slopes of 194 and 204 mV/decade, respectively. From the intercept of the Tafel plot, the geometric area-normalized exchange current density for the  $V^{3/2+}$  couple was calculated as 0.148 and 0.149  $\text{mA}/\text{cm}^2$  (BET-area-normalized  $2.25 \times 10^{-3}$  and  $2.28 \times 10^{-3}$   $\text{mA}/\text{cm}^2$ ) for charging and discharging, respectively. The  $R^2$  values for the linear fits exceeded 0.998, indicating very good correspondence to Tafel behavior for the  $V^{3/2+}$  couple.

However, the positive electrode did not exhibit linear behavior on the Tafel plot. Indeed, the  $V^{5/4+}$  reaction was not sufficiently polarized to reach the Tafel region. In this situation we can estimate the  $j_0$  from the linearized Butler-Volmer expression, allowing a plot of current density against overpotential to yield a slope directly proportional to  $j_0$ .<sup>12</sup> With this approach, the geometric area-normalized exchange current density of 6.48 and 6.65  $\text{mA}/\text{cm}^2$  (BET area-normalized 0.0988 and 0.101  $\text{mA}/\text{cm}^2$ ) for charging and discharging was obtained for the  $V^{5/4+}$  couple ( $R^2$  was 0.9999). Wen et al.<sup>13</sup> found an exchange current density of 0.218  $\text{mA}/\text{cm}^2$  for 0.5 M vanadium at 50% SoC via glassy carbon RDE. The experimental conditions and materials used by Wen et al.<sup>13</sup> can account for the difference in exchange current. Indeed, it is important to note here that the redox process at different carbon materials could exhibit different kinetic behavior. This expectation is at the heart of our desire to carry out these measurements in situ using the exact battery electrode material.

For these materials, we find that the exchange current density for the  $V^{5/4+}$  couple is  $\sim 44$  times greater than the  $V^{3/2+}$  couple. Clearly, the  $V^{5/4+}$  reaction is far more kinetically facile than the  $V^{3/2+}$  reaction. The VRB performance loss was dominated by the negative electrode kinetics. The symmetric cell measurements support the operating full cell measurements with very similar current responses to imposed overpotentials.

Equations 1 and 2 show the overall reactions that occur at the negative and positive electrodes, respectively.



Glancing at equations 1 and 2 can lead to the expectation that the  $V^{5/4+}$  couple should have comparatively worse kinetics due to the more complex reaction involving participation of protons and removal of an oxygen from the  $V^{5+}$  ion while the  $V^{3/2+}$  couple involves a single electron transfer, expected to be a simple outer sphere electron transfer. A more complete understanding of this is outside the scope of this communication. Clearly more detailed work is needed. However, this finding is suggestive relative to catalytic approaches to improving the negative electrode performance.

### Conclusions

Inclusion of a DHE in an operating VRB allowed in-situ kinetics studies to be performed via polarization curve analysis. The negative electrode dominated overpotential at all current densities, including the low-current kinetic region. The  $V^{5/4+}$  exchange current density was 44 times greater than that of the  $V^{3/2+}$  couple, indicating much faster kinetics for the  $V^{5/4+}$  couple. Relatively large kinetic-region losses observed in VRBs can thus be largely attributed to the  $V^{3/2+}$  couple, which also means that catalysis efforts should be focused on this electrode, rather than the  $V^{5/4+}$  couple.

### References

1. L. Joerissen, J. Garche, and C. Fabjan, *J. Power Sources*, **127**, 98 (2004).
2. D. Aaron, Z. Tang, A. B. Papandrew, and T. A. Zawodzinski Jr., *J. Appl. Electrochem.*, **41**, 1175 (2011).
3. M. Gattrell, J. Park, B. MacDougall, J. Apte, S. McCarthy, and C. W. Wu, *J. Electrochem. Soc.*, **151**, A123 (2004).
4. K. J. Kim, M. S. Park, J. H. Kim, U. Hwang, N. J. Lee, G. Jeong, and Y. J. Kim, *Chem. Commun.*, **44**, 5455 (2012).
5. M. P. Manahan, Q. H. Liu, M. L. Gross, and M. M. Mench, *J. Power Sources*, **222**, 498 (2013).
6. D. Aaron, Z. Tang, J. S. Lawton, A. B. Papandrew, and T. A. Zawodzinski, *ECS Trans.*, **41**, 43 (2011).
7. S. C. Barton, Y. Sun, B. Chandra, S. White, and J. Hone, *Electrochemical and Solid-State Letters*, **10**, B96 (2007).
8. G. Li and P. G. Pickup, *Electrochim. Acta.*, **49**, 4119 (2004).
9. J. Zhang, L. Li, Z. Nie, B. Chen, M. Vijayakumar, S. Kim, W. Wang, B. Schwenzer, J. Liu, and Z. Yang, *J. Appl. Electrochem.*, **41**, 1215 (2011).
10. W. He and T. V. Nguyen, *J. Electrochem. Soc.*, **151**, A185 (2004).
11. Z. Liu, J. S. Wainwright, W. Huang, and R. F. Savinell, *Electrochim. Acta*, **49**, 923 (2004).
12. A. Bard and L. Faulkner, *Electrochemical Methods: Fundamentals and Applications*, John Wiley & Sons, New York, 2001.
13. Y. H. Wen, H. M. Zhang, P. Qian, H. P. Ma, B. L. Yi, and Y. S. Yang, *Chin. J. Chem.*, **25**, 278 (2007).